Journal of Power Sources 193 (2009) 864–870

Contents lists available at ScienceDirect

Journal of Power Sources

journal homepage: www.elsevier.com/locate/jpowsour

# Effect of deep discharge on the electrochemical behavior of cobalt oxides and oxyhydroxides used as conductive additives in Ni-MH cells

Myriam Douin[a,b,c], Liliane Guerlou-Demourgues[a,b,*], Lionel Goubault[c], Patrick Bernard[c], Claude Delmas[a,b]

[a] CNRS, ICMCB, 87, Av. Dr. A. Schweitzer, 33608 Pessac Cedex, France
[b] Université de Bordeaux, ICMCB, ENSCPB, F33608 Pessac Cedex, France
[c] SAFT - Direction de la Recherche, 111-113 Boulevard Alfred Daney, 33074 Bordeaux Cedex, France

ARTICLE INFO

*Article history:*
Received 3 December 2008
Received in revised form 18 February 2009
Accepted 15 March 2009
Available online 26 March 2009

*Keywords:*
Alkaline batteries
Cobalt oxide
Sodium cobaltite
Deep discharge

ABSTRACT

When used as conductive additive at the positive electrode of Ni-MH batteries, the $Na_{0.6}CoO_2$ phase is converted, during the first charge, by oxidation, in a γ-hydrated cobalt oxyhydroxide, which exhibits promising performances. The behavior of these phases was studied in specific deep discharge or low potential storage conditions, through electrochemical short-circuit experiments. The evolution of the electrodes during the cycling was followed by X-ray diffraction and SEM analysis. These novel additives appear to be more efficient in these extreme conditions than the CoO or $Co(OH)_2$ additives, commonly used in industrial devices.



## 1. Introduction

In Ni-MH batteries, the current technology of pasted positive electrodes needs to use conductive additives, since the electrochemical active material, $Ni(OH)_2$, exhibits a poor electronic conductivity [1,2]. CoO cobalt oxide or $Co(OH)_2$ cobalt oxyhydroxide, which are usual additives, are transformed, during the first charge, into a conductive $H_xCoO_2$ type phase [3,4]. This one is unstable at low voltages; it is indeed reduced into $Co(OH)_2$, which is soluble in the electrolyte, leading to a degradation of the conductive network and a capacity loss of the battery [5–7]. That is the reason why research works are now devoted to new additives, to prevent the instability of the conductive network. The addition of bismuth to the cobalt phases [8] or the use of a conductive $H_xLi_yCo_{3-\delta}O_4$ spinel type phase, formed in situ under specific conditions [9–11], are solutions proposed in literature.

In this context, the effect of the $Na_{0.6}CoO_2$ phase, as conducting additive to $Ni(OH)_2$, has been investigated in our lab. This layered oxide is a promising conductive additive, thanks to its metallic electronic conductivity and its good stability in the potential range of Ni-MH batteries. Preliminary works of Tronel et al. have shown, in our lab, a good efficiency of the additive, even at low potential [12].

This study was motivated by the registration, by Japanese battery manufacturers, of several patents, which underlined the beneficial effect of sodium on the stabilisation of the cobalt conductive subnetwork [13–15]. Tronel et al. have shown that the $Na_{0.6}CoO_2$ phase is transformed, after few cycles within the electrode, into a γ-type hydrated cobalt oxyhydroxide [16]. This latter phase, formed in situ, is a promising candidate because it exhibits a slow reduction kinetics in concentrated alkaline electrolyte [17].

The usual method, employed to test "resistance" of the battery with regard to a deep discharge or a long storage in discharged state, consists in keeping the cell, at the end of a discharge, in short-circuit on a resistor during several days. The present paper aims at comparing, in these conditions, the behaviors and the evolutions of the $Na_{0.6}CoO_2$ phase and deriving γ-type cobalt oxyhydroxides with those of the usual $Co(OH)_2$ additive, which is known to entail a loss of efficiency of the conductive network in such conditions.

## 2. Experimental

### 2.1. Synthesis of the conductive additives

The $Na_{0.6}CoO_2$ phase is synthesized by solid-state reaction from $Co_3O_4$ and $Na_2O$ (12 wt.% excess) oxides in a tubular furnace, at 550 °C, during 15 h, under oxygen flux [18]. The $Co_3O_4$ precursor is obtained by decomposition of $CoCO_3$, during 12 h, at 440 °C, under flowing $O_2$.

* Corresponding author at: CNRS, ICMCB, 87, Av. Dr. A. Schweitzer, 33608 Pessac Cedex, France. Tel.: +33 5 40 00 27 25; fax: +33 5 40 00 66 98.
*E-mail address:* guerlou@icmcb-bordeaux.cnrs.fr (L. Guerlou-Demourgues).

0378-7753/$ – see front matter © 2009 Elsevier B.V. All rights reserved.
doi:10.1016/j.jpowsour.2009.03.031

Three different processes are used to prepare γ-cobalt oxyhydroxide phases (denoted as γ-Co in the following) from $Na_{0.6}CoO_2$. The first method consists of an oxidizing hydrolysis, which is performed by introducing 1 g of $Na_{0.6}CoO_2$ in 200 mL of a 4 M KOH–0.8 M NaClO solution [4]. After a 15-h stirring, the material is recovered by centrifugation, rinsed in deionised water and dried 15 h at 60 °C. The second technique used consists of an electrochemical oxidation of the $Na_{0.6}CoO_2$ phase. 3 g of $Na_{0.6}CoO_2$ is trapped, by mechanical pressure, between two pieces of nickel foam. The so-constituted electrode is "sandwiched" between two cadmium electrodes. The cell is immersed into an 8 M KOH electrolyte. After a 20-h soaking, the cell is charged for 5 h at the *C*/20 rate. (The theoretical capacity "*C*" of the battery is calculated on the basis of one electron exchanged per cobalt atom.) Then, the positive electrode is removed, rinsed in deionised water and dried for 15 h at 60 °C. The two pieces of nickel foam of the electrode are simply unsticked one of each other, to recover the cobalt material. Finally, the third method that is used to obtain a γ-Co phase consists in ageing the $Na_{0.6}CoO_2$ phase, during one month, in 8 M KOH electrolyte. Such treatment leads to spontaneous transformation of $Na_{0.6}CoO_2$ into a mixture of a majority γ-Co type phase and of a β(III) type phase, as described in a previous paper [17].

### 2.2. Preparation of the cells

Electrodes for electrochemical experiments are prepared by mixing 2/3 of $Ni(OH)_2$ active material (OMG E148309-1 nickel hydroxide, containing small amounts of syncrystallized cobalt and zinc) and 1/3 of studied conductive material (weight fraction). 1 wt.% "powdered" PTFE is then added as a binder. 200 mg of the mixture is pasted on a nickel foam (1 cm × 4 cm), which play both the roles of electrode support and current collector. The so-constituted positive electrode is pressed at 1 t $cm^{-2}$, wrapped into a non-woven tissue and then positioned between two polyvinyl chloride plates. Two sintered cadmium hydroxide electrodes are placed on both sides of the positive electrode. Their capacity is strongly exceeding that of the positive electrode, so as not to play a limiting role with regard to the cycling of the battery. The cadmium electrode plays also the role of reference electrode, so that all potential values are given in this paper versus $Cd(OH)_2$/Cd potential. The cell is immersed in an 8 M KOH electrolyte solution.

### 2.3. Characterization

A galvanostatic cycling is started about 18 h after the addition of the electrolyte. The first cycle consists of a charge, for 20 h, at the *C*/10 rate, followed by a discharge, down to 0.9 V, at the *C*/5 rate (the theoretical capacity "*C*" of the battery is calculated on the basis of one electron exchanged per nickel atom.) Then, the cycling process consists in alternating 6-h charges and discharges down to 0.9 V, at the *C*/5 rate. In the middle of the cycling, a low potential storage test is carried out by performing a short-circuit of the cell on a 10 Ω resistance, during 3 days. The classical cycling at the *C*/5 rate is afterwards started again (up to 60 cycles).

X-ray diffraction (XRD) data are collected with a PANalytical X'pert Pro diffractometer, using the Kα Co radiation. The diffraction patterns are recorded in the [5–110°] (2$\theta$) angular range, using a 0.0167° (2$\theta$) step, with an active length of 2.122° in the detector and a constant counting time of 100 s per step. XRD characterizations of the electrode materials are systematically performed in the discharged state. Let us note that, when XRD analysis is performed directly on the electrode, no special care is taken in terms of sample preparation; the rules of isodensity and random disorientation of crystallites are therefore not systematically matched. Consequently, XRD patterns give qualitative but not quantitative information: the relative intensity of the diffraction lines, corresponding to two phases in a sample, cannot be directly compared.

Scanning electron micrographs are collected with a Hitachi S-4500 field emission microscope, with an accelerating voltage of 3.0 kV, in secondary electrons mode.

Temperature-dependent electronic conductivity measurements are carried out with the four-probe technique [19], using a direct current. Because of the low-temperature synthesis, the studied material could not be sintered. For this reason, pellets (8 mm of diameter and approximately 1.2 mm in thickness) are only obtained by compacting 200 mg of powder, at 8 t $cm^{-2}$, under vacuum.

Inductively coupled plasma (ICP) spectrometry, performed at SAFT laboratory, in Bordeaux (France), was used for Na, K, and Co titrations. The oxidation state of cobalt was determined in the laboratory by the iodometric titration method [11].

## 3. Electrochemical performances of the cobalt conductive additives

### 3.1. Conductive additives studied

In the present paper, five cobalt phases are studied as conductive additive at the positive electrode of Ni-MH battery: $Na_{0.6}CoO_2$, the three derivative γ-Co phases, obtained in different synthesis conditions (as described in Section 2.1), and $Co(OH)_2$, which, commonly used in industrial devices, plays the role of reference additive. Table 1 summarises the chemical compositions and the average oxidation degree of cobalt in these synthesized four materials. Comparison of the chemical compositions of the three γ-Co derivatives materials with the composition of the $Na_{0.6}CoO_2$ precursor phase shows the exchange of a majority part of the sodium ions by potassium ions, which occurs simultaneously with insertion of water molecules [17].

As these materials are intended to be used as conductive additives, their electronic conductivity was examined. The curves are presented in Fig. 1, while conductivity and activation energy values at room temperature are reported in Table 1.

The $Na_{0.6}CoO_2$ and the γ-Co phases, obtained by chemical or electrochemical oxidation, exhibit high conductivity with a metallic behavior, whereas the material obtained by ageing presents a lower conductivity. Let us remember that, as mentioned in Section 2.1, this latter phase is biphasic, containing a γ-Co type and a β(III)-

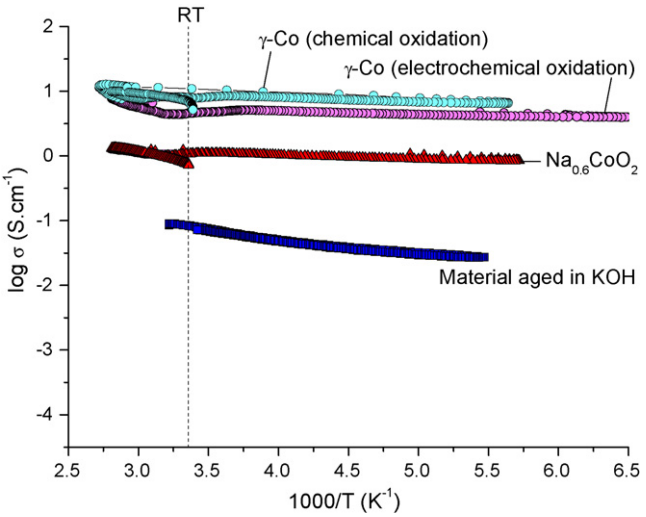


**Fig. 1.** Variation of the logarithm of electrical conductivity versus reciprocal temperature for the $Na_{0.6}CoO_2$ phase and the derived γ-Co phases, obtained by ageing in KOH, electrochemical oxidation or chemical oxidation from $Na_{0.6}CoO_2$.

**Table 1**
Comparison of chemical compositions, average oxidation states of cobalt, conductivity and activation energy values at room temperature, for the studied conductive additives: $Na_{0.6}CoO_2$, the material obtained by ageing in KOH, γ-Co obtained by electrochemical oxidation and γ-Co obtained by chemical oxidation from the $Na_{0.6}CoO_2$ phase.

| | Co (wt.%) | K (wt.%) | Na (wt.%) | Ox. degree of cobalt | $\sigma$ (298 K) (S cm$^{-1}$) | $E_a$ (298 K) (eV) |
|---|---|---|---|---|---|---|
| $Na_{0.6}CoO_2$ | 56.0 | – | 12.9 | 3.4 | 1.1 | 0.005 |
| Material aged in KOH | 49.4 | 11.1 | 3.1 | 3.4 | $8 \times 10^{-2}$ | 0.05 |
| γ-Co (electrochemical oxidation) | 52.0 | 8.9 | 2.2 | 3.6 | 5.7 | 0.007 |
| γ-Co (chemical oxidation) | 54.5 | 9.7 | 1.7 | 3.6 | 9.5 | 0.003 |

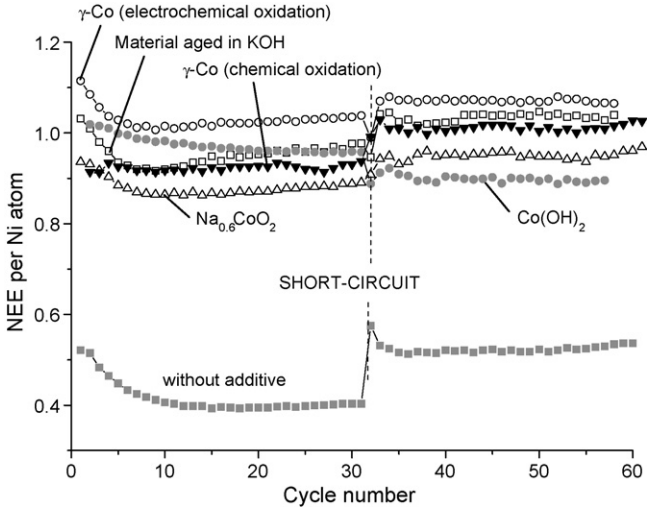


**Fig. 2.** Evolution of the number of electron exchanged per nickel atom, for electrodes containing $Ni(OH)_2$, without any additive or with 33% conductive material added. The 5 additives studied were: reference $Co(OH)_2$, $Na_{0.6}CoO_2$, the material obtained after ageing in KOH, and the γ-Co phases, obtained by electrochemical oxidation or chemical oxidation from $Na_{0.6}CoO_2$.

Co type phase [17]; the semi-conductor character of the β(III)-Co component is the reason for the difference with the other studied γ-Co phases.

The metallic character of $Na_{0.6}CoO_2$ and the γ-Co phases is due to an overlapping of the cobalt $t_{2g}$ orbitals, across the shared edges of the $CoO_6$ octahedra, in $CoO_2$ slabs. It leads to electronic delocalization within cobalt slabs, which is possible thanks to the presence of $Co^{4+}$ ions ($t_{2g}^5 e_g^0$) and to a short distance between two cobalt atoms ($d_{Co-Co}$ = 2.82 Å), lower than the critical Goodenough radius [20] ($R_c$ = 2.885 Å).

**Table 2**
Number of electron exchanged per nickel atom before and after short-circuit, depending on the conductive additive used: $Co(OH)_2$, $Na_{0.6}CoO_2$, material aged in KOH, γ-Co obtained by electrochemical oxidation, γ-Co obtained by chemical oxidation from $Na_{0.6}CoO_2$.

| | Before short-circuit | After short-circuit | Percentage difference |
|---|---|---|---|
| Without additive | 0.4 | 0.50 | +25% |
| $Co(OH)_2$ | 0.95 | 0.90 | −7% |
| $Na_{0.6}CoO_2$ | 0.85 | 0.95 | +12% |
| Material aged in KOH | 0.90 | 0.95 | +6% |
| γ-Co (electrochemical oxidation | 1.00 | 1.05 | +5% |
| γ-Co (chemical oxidation) | 0.90 | 0.95 | +12% |

### 3.2. Results of electrochemical tests

Fig. 2 allows to compare the electrochemical behaviors of the various phases, $Na_{0.6}CoO_2$ and deriving phases, as conductive additives to $Ni(OH)_2$ active material. The number of electrons exchanged (NEE) per nickel atom is displayed as a function of the cycle number. Whatever the conductive material added, the cells exhibit good capacities with a NEE close to 1, which has to be compared with the cell without any additive, which allows to recover only 40% of the theoretical capacity.

After 30 cycles, the batteries were subjected to a short-circuit test, as described in Section 2, simulating a deep discharge or a long storage at the discharged state of the cell. The values of the NEE before and after the short-circuit test, for each conductive material, are reported in Table 2.

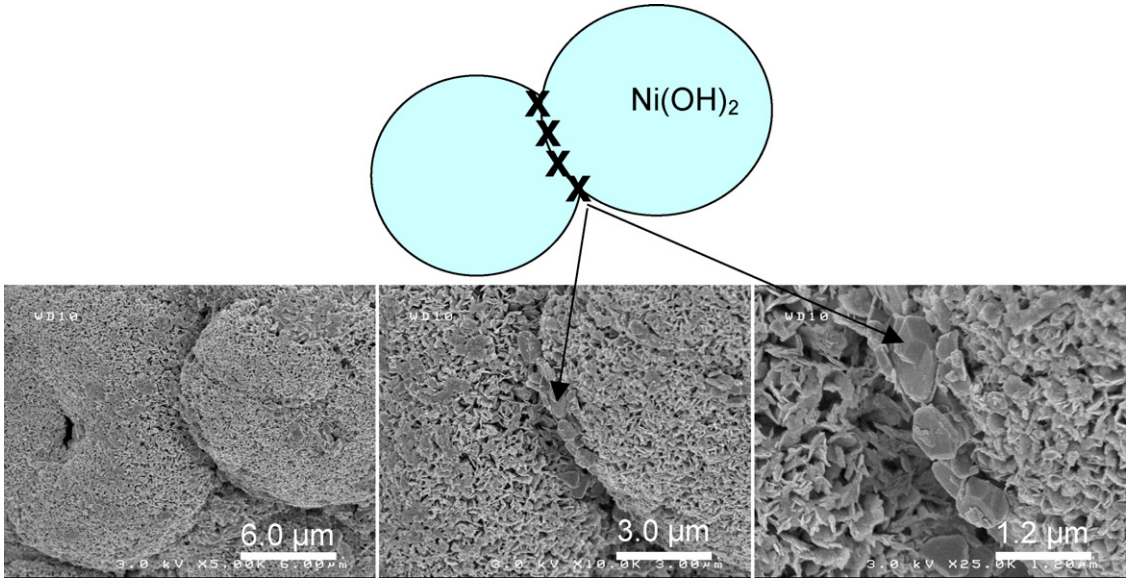


**Fig. 3.** SEM pictures of $Na_{0.6}CoO_2$ particles, distributed at the junction of two spherical agglomerates of nickel hydroxide crystallites.

With the $Co(OH)_2$ cobalt hydroxide, the reference conductive additive, the capacity of the battery decreases of 7% after the short-circuit test. This known behavior illustrates the instability, at low potential, of the conductive $H_xCoO_2$ phase [4], formed during the first charge. As explained in Section 1 the introduction, the conductive phase is reduced into $Co(OH)_2$, which tends to be dissolved in the electrolyte, leading to damage the conductive network; the active material does not completely work any longer, which results in a decrease of the cell capacity.

For all other conductive materials added, the capacity of the battery exhibits an increase (5–12%) after the short-circuit test. Very surprisingly, the cell without additive shows similar behavior, with a high increase of the capacity (+25%). Such behavior will be investigated in a forthcoming paper, it may be due to partial redistribution of the active matter during the short-circuit.

In order to investigate the phenomena, which occurred in the material during the short-circuit experiment, the evolution of the additive materials was followed through XRD and SEM analysis of the electrodes, all along the cycling process.

## 4. Evolution of the texture of the NOE

Aiming at studying the evolution of the nickel oxide electrode during the cycling process, depending on the cobalt phase added, 4 identical cells, containing a same additive phase, are cycled simultaneously and stopped at different times of the cycling experiment: after soaking in 8 M KOH electrolyte for one night, after about 30 cycles, after the short-circuit test for 3 days on a resistor, and at the end of the cycling. Each time, the electrode is rinsed with deionised water, dried at 60 °C and analysed by XRD and SEM.

As an illustration, Fig. 3 presents SEM pictures of the nickel electrode with the $Na_{0.6}CoO_2$ additive: cobalt plates are distributed at the junction of two spherical agglomerates, which are constituted of primary crystallites of nickel hydroxide. Thanks to its ideal distribution, the additive material can fully play its role of conductive additive, by collecting electrons, exchanged at every nickel hydroxide sphere. Let us note that, in the following, pictures are focused on plates of cobalt conductive additive, rather than on nickel hydroxide particles.

### 4.1. With the $Co(OH)_2$ reference additive

Figs. 4 and 5 present X-ray diffraction and SEM analysis results, obtained for $Ni(OH)_2$ electrodes with reference $Co(OH)_2$ added. In the initial state, the lines, characteristic of β(II)-$Ni(OH)_2$ and β(II)-$Co(OH)_2$, are present. After soaking of the electrode in the electrolyte, the diffraction lines of β(II)-$Co(OH)_2$ disappear, while a shoulder appears on the right of the (0 0 1) line of $Ni(OH)_2$, which can be attributed to the (0 0 3) line of a β(III)-Co type phase, formed by oxidation of $Co(OH)_2$ by air. As expected, the β(III)-Co phase continues to grow and remains stable during the cycling. SEM pictures of the electrode, obtained after 30 cycles, are presented in Fig. 5, show that the cobalt material exhibits two types of morphology: plate-shaped particles, analogous with the initial morphology (Fig. 5a) and thin flakes (Fig. 5b). Pralong et al. claimed that cobalt oxyhydroxides can exhibit different textures, depending on the experimental conditions of oxidation (charging rate in particular) of $Co(OH)_2$ into CoOOH [22]. The texture observed in Fig. 5a may correspond to oxidation within the solid state, while the new texture, observed in Fig. 5b, is significantly different from that of the initial plates and corresponds to a dissolution/precipitation process of the cobalt phase. As known, $Co(OH)_2$ is transformed during the first charge into a highly conductive $H_xCoO_2$ oxyhydroxide, which ensures a good capacity for the battery [2,3,21]. The transformation occurs in situ through a dissolution/precipitation process via the formation of a blue Co(II) complex ion [2].

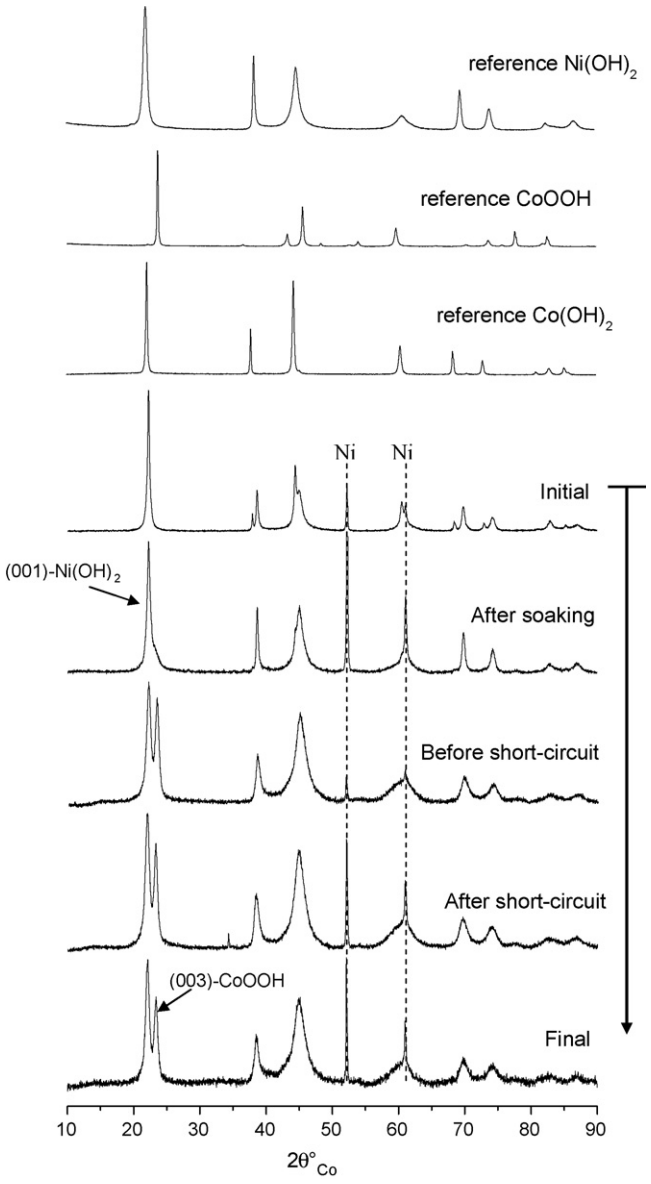


**Fig. 4.** Evolution of the XRD patterns of an electrode containing $Ni(OH)_2$ with 33% $Co(OH)_2$ added, at different times of the cycling process: at the initial state, after soaking, after 30 cycles just before short-circuit, after short-circuit and at the end of the cycling process.

After the short-circuit, simulating deep discharge, no significant difference can be observed on the X-ray diagrams (Fig. 4). Such result could seem contradictory to the expected partial reduction of the $H_xCoO_2$ conductive phase into β(II)-$Co(OH)_2$, normally at 0.67 V [6]. The β(II)-$Co(OH)_2$ can actually not be observed for two main reasons: first, it is dissolved within the electrolyte at low potential [23] and second, it can be spontaneously oxidized into stoichiometric β(III)-CoOOH [24] by air, when the electrode is removed from the electrolyte and prepared for X-ray diffraction experiment.

### 4.2. With the $Na_{0.6}CoO_2$ and γ-type phases as conductive additives

Fig. 6 presents the X-ray diffraction patterns of electrodes containing 33 wt.% $Na_{0.6}CoO_2$, added to $Ni(OH)_2$, and stopped at different points of the cycling process. After 18 h soaking of the

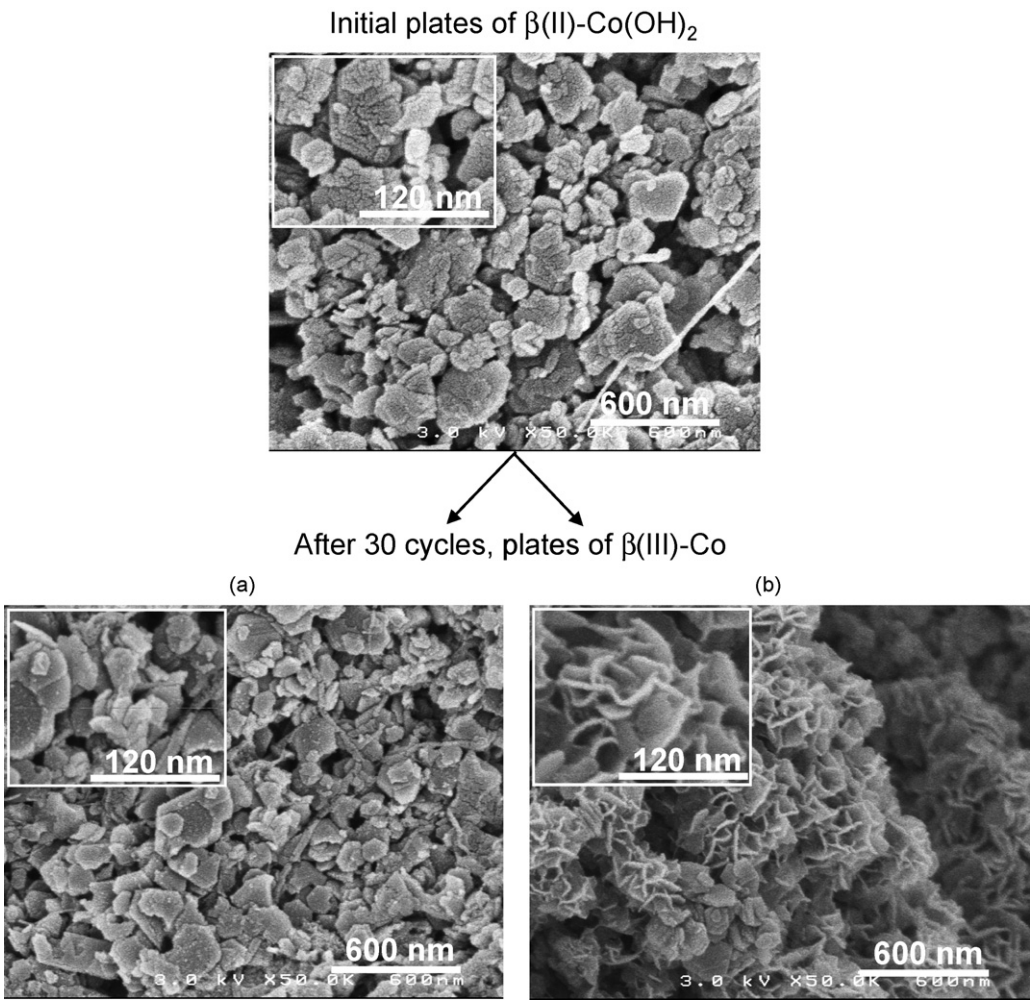


**Fig. 5.** SEM pictures, focused on the cobalt additive, in an electrode containing $Ni(OH)_2$ with 33% $Co(OH)_2$ added, at the initial state and after 30 cycles. The two types of morphology (a) and (b) were observed on the same cycled electrode.

electrode in the electrolyte, the diffraction lines, related to the nickel hydroxide phase are not modified, whereas an interstratified cobalt phase, characterized by a wide and dissymmetric peak at low angles (* in Fig. 6), appears. The distance that corresponds to this wide peak (around 6.67 Å) is intermediate between the distances that are observed for the (0 0 3) lines of $Na_{0.6}CoO_2$ ($d$(0 0 3) = 5.51 Å) and γ-Co ($d$(0 0 3) = 6.85 Å). The presence of such an interstratified phase is in accordance with the results obtained during the specific study of the evolution of $Na_{0.6}CoO_2$ in KOH solution [17]. This work highlighted, thanks to ageing tests, a spontaneous transformation of $Na_{0.6}CoO_2$ into γ-Co, with a mechanism of exchange of alkaline ions in interslab space. This transformation is progressive and takes place via the formation of an interstratified phase.

After about thirty cycles (just before the short-circuit experiment), the $Na_{0.6}CoO_2$ phase has completely disappeared, at the expense of a γ-Co phase. Indeed, it should be noticed that the line observed at about 6.83 Å ($2\theta = 15^\circ$) can be unambiguously assigned to a γ-Co phase ((0 0 3) line), rather than to γ-Ni oxyhydroxide phase, because of its narrow width. The γ-Co phase that appeared during cycling remains stable after short-circuit, which confirms its good stability in cycling, as already claimed by Tronel et al. [16].

SEM analysis has been performed on these electrodes. Several representative pictures, focused on cobalt materials, are shown in Fig. 7. At the initial state, the plates of $Na_{0.6}CoO_2$ are distributed around the nickel hydroxide agglomerate spheres. During the cycling process, the microstructure of the additive material is almost not altered, which is in accordance with its stability. In particular, the thin flakes texture, characteristic of precipitated β(III)-Co (as presented in Fig. 5b), is not observed.

Similar investigation has been performed on electrodes containing the other studied materials (the $Na_{0.6}CoO_2$ phase, aged in electrolyte, and the γ-Co phases, obtained by electrochemical or chemical oxidation of $Na_{0.6}CoO_2$). The X-ray diffraction and SEM results are not presented here because, for all the three cases, the behavior is quite similar to that observed for pristine $Na_{0.6}CoO_2$.

## 5. Effect of short-circuit on the electrochemical behavior of the cobalt conductive additives

The aim of the experiments, reported in this paragraph, is to compare the behavior of γ-Co and β(III)-Co, which are the conductive materials formed in situ, from $Na_{0.6}CoO_2$ and from reference $Co(OH)_2$ respectively, in relation to short-circuit and to their "resistance" to deep discharge. For this purpose, short-circuit test was performed on electrodes containing only cobalt phases, without nickel hydroxide, contrarily to Section 4, in which electrodes were containing $Ni(OH)_2$ together with the cobalt additives.

In a first step, the absence of any influence of the nickel foam on the increase of the cell capacity observed after short-circuit was checked. The metallic nickel foam is indeed both the support and the current collector of the electrode. In order to know if foam nickel

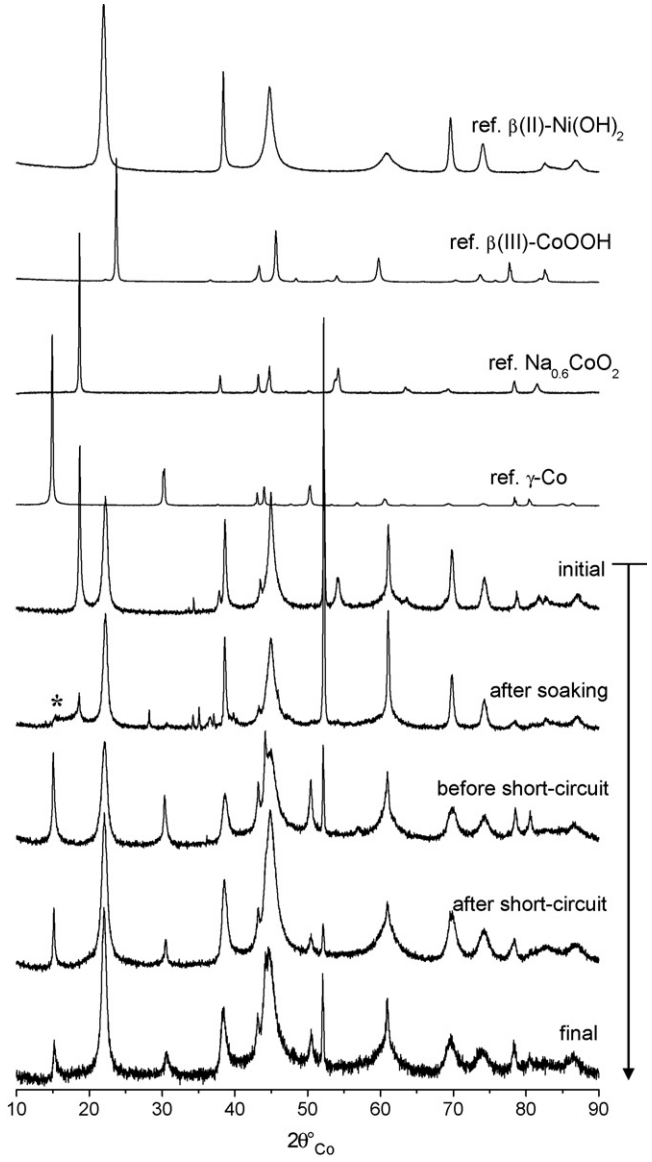


**Fig. 6.** Evolution of the XRD patterns of an electrode containing $Ni(OH)_2$ with 33% $Na_{0.6}CoO_2$ added, at different times of the cycling process: at the initial state, after soaking in electrolyte, after 30 cycles just before short-circuit, after short-circuit and at the end of the cycling process.

could significantly take part to cell capacity, a cycling process with short-circuit test was carried out on a single foam. The X-ray diffraction pattern of metallic nickel foam after cycling (not presented here) does not show any difference with that before cycling. No nickel hydroxide phase, which could be formed from oxidation of the nickel foam, or from NiO thin film present on the surface, was observed. Therefore, the metallic nickel foam cannot be considered as responsible for the capacity increase that is observed after the short-circuit.

The electrodes containing either $Na_{0.6}CoO_2$ or $Co(OH)_2$, without nickel hydroxide, were charged before the short-circuit test (the theoretical capacity of the cells was calculated on the basis of one electron exchanged per cobalt atom). The $Na_{0.6}CoO_2$ based cell was charged for 5 h, at the *C*/20 rate, to remove 0.25 electrons per cobalt atom, which is necessary to oxidize $Na_{0.6}CoO_2$ into γ-Co [17]. The $Co(OH)_2$ based cell was in turn charged for 6 h, at the *C*/5 rate, to remove 1 electron, and reach therefore β(III)-Co. Fig. 8 allows us to compare the XRD patterns of the cells after short-circuit (for clarity reasons, the diagrams of the γ-Co and β(III)-Co obtained after oxidation were not reported in Fig. 8, they were identical to those reported in Figs. 6 and 4 just before short circuit). The X-ray diagram of the $Co(OH)_2$ based electrode just after short circuit shows a mixture of β(II)-Co and β(III)-Co cobalt oxides, which is an evidence for the reduction of β(III) into β(II) during the short circuit. As indicated in Fig. 8 by dotted lines, the diagram of the $Na_{0.6}CoO_2$ based electrode presents a mixture containing γ-Co, β(III)-Co and an interstratified phase. Such interstratified phase, already described in Section 4.2, was reported to consist of a random stacking of γ-Co and β(III)-Co planes, resulting from partial

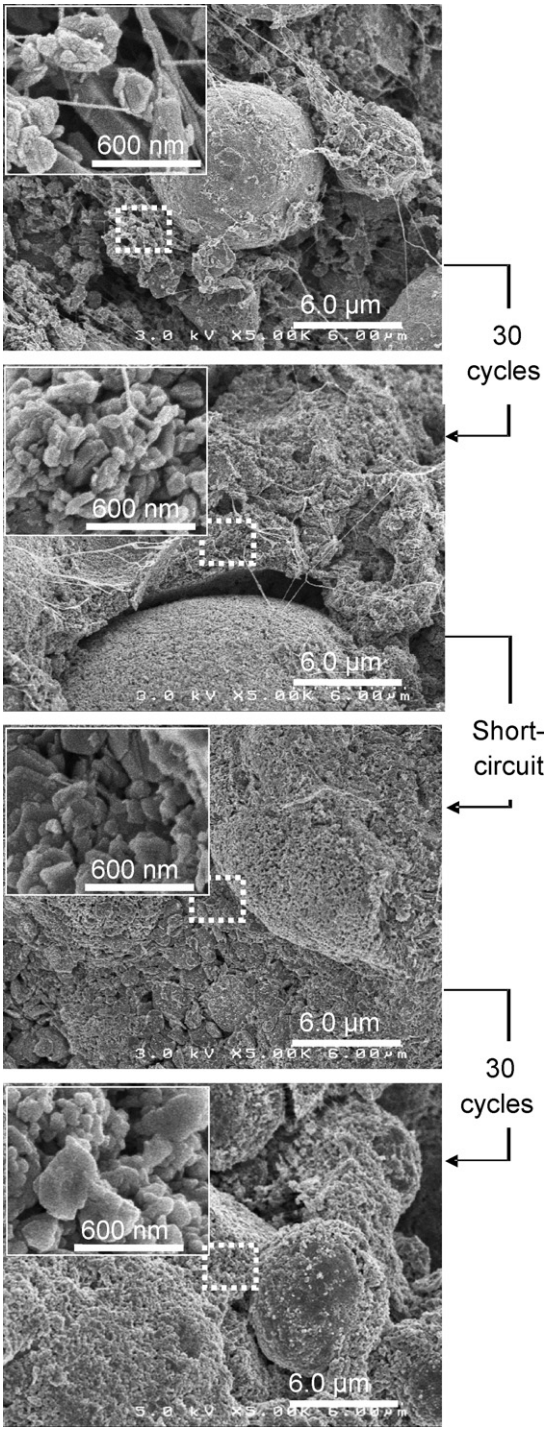


**Fig. 7.** SEM pictures of an electrode containing $Ni(OH)_2$ with 33% $Na_{0.6}CoO_2$ added, at different times of the cycling process: at the initial state, after 30 cycles just before short-circuit, after short-circuit and at the end of the cycling process. PTFE threads can be observed on some pictures.

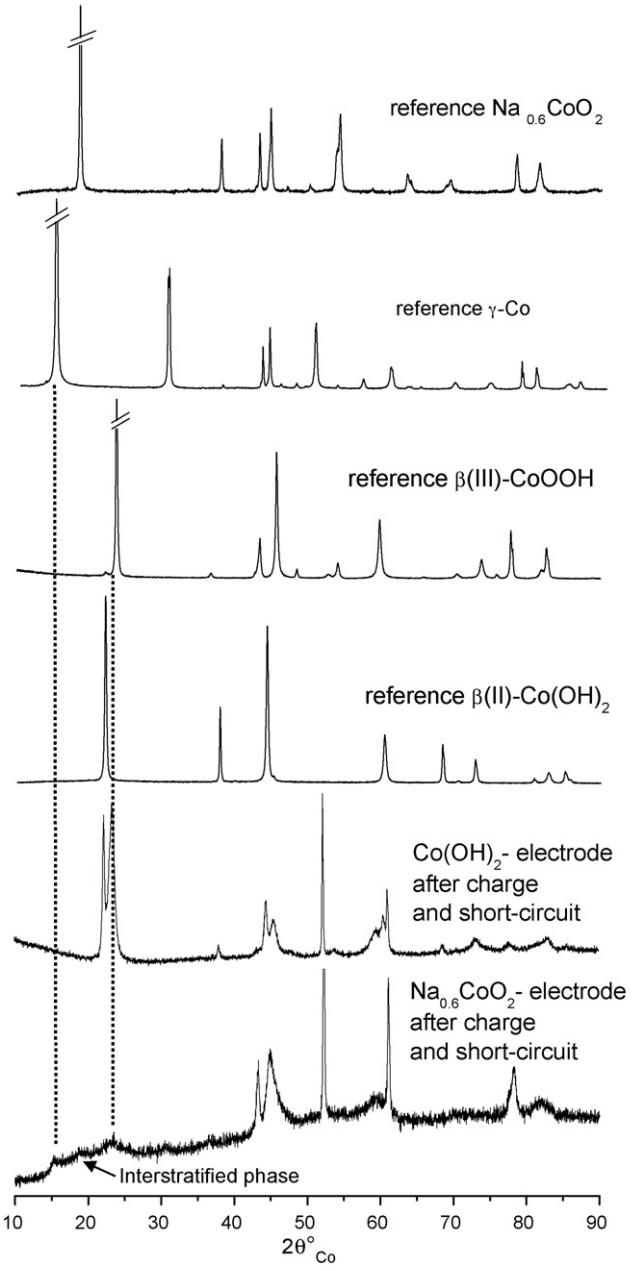


**Fig. 8.** X-ray diffraction patterns of $Na_{0.6}CoO_2$ and $Co(OH)_2$ based electrodes, charged and subjected to a short-circuit test.

reduction of some γ-Co planes into β(III) ones [17]. The fact that the reduction of γ-Co passes through an intermediate interstratified phase, before reaching β(III)-Co, is in favour of the higher stability of γ-Co with regard to β(III)-Co, in deep discharge conditions. This should be due to lower reduction kinetics of the γ-Co phase, as compared with β(III)-Co.

## 6. Conclusion

In the presence of additive cobalt phases ($Na_{0.6}CoO_2$, hydrated cobalt oxyhydroxides and reference $Co(OH)_2$), 90–100% of the $Ni(OH)_2$ active material is electrochemically working. The cell behaviors are similar with our $Na_{0.6}CoO_2$ or γ derivative phases. During a deep discharge, the cobalt phases are indeed not reduced into β(III)-CoOOH (then β(II)-$Co(OH)_2$), thanks to a slow reduction kinetics. Nevertheless, they can be reduced into an interstratified phase, characterized by a random stacking of γ and β(III) planes, which are reoxidized into γ-Co during the subsequent charge. The integrity of the conductive network is therefore maintained, contrarily to what happens with the $H_xCoO_2$ phase, formed from the $Co(OH)_2$ reference additive.

## Acknowledgements

The authors wish to thank C. Denage and P. Dagault for technical assistance, E. Lebraud and S. Pechev for X-ray diffraction, R. Decourt for conductivity measurements and O. Guiader (SAFT) for ICP titration. SAFT, ANRT and Region Aquitaine are acknowledged for their financial support.

## References

[1] M. Oshitani, M. Watada, T. Tanaka, T. Iida, Electrochem. Soc. Proc. Ser. (1994) 303.
[2] M. Oshitani, H. Yufu, K. Takashima, S. Tsuji, Y. Matsumaru, J. Electrochem. Soc. 136 (6) (1989) 1590–1593.
[3] P. Benson, G.W.D. Briggs, W.F.K. Wynne-Jones, Electrochim. Acta 9 (1964) 281–288.
[4] M. Butel, L. Gautier, C. Delmas, Solid State Ionics 122 (1999) 271–284.
[5] L. Gautier, Thesis University of Bordeaux I, France, 1995.
[6] V. Pralong, A. Delahaye-Vidal, B. Beaudoin, J.B. Leriche, J.M. Tarascon, J. Electrochem. Soc. 147 (4) (2000) 1306.
[7] V. Pralong, Y. Chabre, A. Delahaye Vidal, J.M. Tarascon, Solid State Ionics 147 (1–2) (2002) 73–84.
[8] V. Pralong, A. Delahaye Vidal, B. Beaudoin, J.B. Leriche, J. Scoyer, J.M. Tarascon, J. Electrochem. Soc. 147 (6) (2000) 2096–2103.
[9] M. Douin, L. Guerlou-Demourgues, M. Ménétrier, E. Bekaert, L. Goubault, P. Bernard, C. Delmas, Chem. Mater. 20 (2008) 6880–6888.
[10] M. Douin, L. Guerlou-Demourgues, M. Ménétrier, E. Bekaert, L. Goubault, P. Bernard, C. Delmas, J. Solid State Chem., in press, doi:10.1016/j.jssc.2009.02.018.
[11] F. Tronel, L. Guerlou-Demourgues, M. Ménétrier, L. Croguennec, L. Goubault, P. Bernard, C. Delmas, Chem. Mater. 18 (25) (2006) 5840–5851.
[12] F. Tronel, Thesis University of Bordeaux I, France, 2003.
[13] F. Kato, F. Tanigawa, Y. Dansui, K. Yuasa, EP 0851516, 1998.
[14] A. Yamawaki, S. Nakahori, T. Hamamatsu, Y. Baba, EP 0757395, 1997.
[15] T. Tanaka, J. Imaizumi, T. Iida, JP2001052695, 2001.
[16] F. Tronel, L. Guerlou-Demourgues, M. Basterreix, C. Delmas, J. Power Sources 158 (1) (2006) 722–729.
[17] M. Douin, L. Guerlou-Demourgues, L. Goubault, P. Bernard, C. Delmas, J. Electrochem. Soc., in press.
[18] C. Fouassier, G. Matejka, J.M. Reau, P. Hagenmuller, J. Solid State Chem. 6 (1973) 532–537.
[19] J. Laplume, L'onde électrique 335 (1955) 113–125.
[20] R.G. Egdell, J.B. Goodenough, A. Hammett, C.C. Naish, J. Chem. Soc. 79 (1983) 983.
[21] M. Butel, Thesis University of Bordeaux I, France, 1998.
[22] V. Pralong, A. Delahaye-Vidal, B. Beaudoin, B. Gérand, J.M. Tarascon, J. Mater. Chem. 9 (1999) 955.
[23] P. Benson, G.W.D. Briggs, W.F.K. Wynne-Jones, Electrochim. Acta 9 (1964) 275–280.
[24] S. Le Bihan, M. Figlarz, J. Cryst. Growth 13–14 (1972) 458.